Pure Appl. Chem., Vol. 83, No. 4, pp. 869–883, 2011.
doi:10.1351/PAC-CON-10-09-32

Laser-trapping assembling dynamics of molecules and proteins at surface and interface*

Hiroshi Masuhara[1,2,‡], Teruki Sugiyama[1], Thitiporn Rungsimanon[1], Ken-ichi Yuyama[1], Atsushi Miura[2], and Jing-Ru Tu[2]

[1]Graduate School of Materials Science, Nara Institute of Science and Technology, Ikoma 630-0192, Japan; [2]Department of Applied Chemistry and Institute of Molecular Science, National Chiao Tung University, Hsinchu 30100, Taiwan

Abstract: Laser trapping of molecules and proteins in solution at room temperature is made possible by irradiating 1064-nm continuous-wave (CW) laser with power around 1 W. Although conventional small molecules are not trapped at the focal point, molecules that can form clusters upon assembling and proteins whose size is close to 10 nm are gathered, giving unique assembly structure. Glycine in H_2O shows crystallization, urea in D_2O gives a millimeter-sized giant droplet, and cobalt oxide-filled ferritin protein confirms assembly followed by precipitation. Solute concentration, solvent, and laser power are important factors for determining trapping and assembling phenomena, and the laser focal position is very critical. These unique behaviors are realized by setting the irradiation at the air/solution surface, inside the solution, and at the glass/solution interface. Laser trapping-induced crystallization, liquid/liquid phase separation, and precipitation are compared with the previous results and considered. After summarizing the results, we describe our future perspective and plans.

Keywords: assembly formation; glycine; laser trapping; protein; urea.

INTRODUCTION

The laser has been greatly contributing to the development of modern chemistry since its invention in 1960. Studies on laser spectroscopy and photochemistry started from isolated molecules in gas phase and in dilute solution, then shifted to more complex molecules, molecular aggregates, polymers, and supramolecules, and furthermore extended to colloids and molecular solids. The development of photochemistry from homogeneous to inhomogeneous systems has led to the combination of lasers with optical microscopes [1–3]. In the late 1980s, near-field optics and super-resolution imaging were still beyond the knowledge of chemists, so that the combination led to picosecond time- and micrometer space-resolved spectroscopy and chemistry. Indeed, laser-based microchemistry was a pioneering area, while only micro total-analysis-system and micro-electrochemistry allowed chemical processes to be controlled in space. This stream of laser microchemistry has been developing to nanometer dimensions, which is followed in our case as in the books and proceedings [4–8].

*Paper based on a presentation made at the XXIII[rd] IUPAC Symposium on Photochemistry, Ferrara, Italy, 11–16 July 2010. Other presentations are published in this issue, pp. 733–930.

‡Corresponding author

Utilization of intense lasers and microscopes brought about the experimental conditions of high-intensity excitation of molecular materials, leading to multiphoton absorption, ionization, local heating, and eventually decomposition and fragmentation. Nonlinear photophysical processes, photochemical reaction, and laser ablation are quite easily induced under microscope, while only nonlinear optical phenomena are observed in the case of no absorption. One of the well-known phenomena is laser trapping and laser tweezers which are very useful to manipulate micrometer-sized objects, particularly, living cells in solution at room temperature. However, they did not receive much attention from chemists, as they cannot induce reactions and are not efficient to form molecular assemblies. We combined systematically this laser manipulation with spectroscopy, electrochemistry, photopolymerization, and ablation, by which we demonstrated high potential of laser manipulation in space-resolved chemistry and summarized our results as the chemistry of single-micrometer particles and droplets [3].

The minimum size of the objects which can be trapped with a few hundred W of CW 1064-nm laser is a few nm for gold nanoparticle and 8 nm for polystyrene sphere. Actually, a single molecule cannot be trapped, and its diffusion in the focal volume is only a little affected, which is called biased diffusion. Therefore, as nanochemistry, we started to apply laser manipulation technique to polymers in solution as its effective diameter is usually 10 nm or larger [6]. Actually, laser trapping was successful, and the polymers were gathered and formed a visible-size micrometer particle. Their assembling rate was considered as functions of the mean degree of polymerization and chemical structures. The minimum size was determined to be a few nm and π-electronic chromophores are more efficiently trapped because they are more polarizable under high electric field. Therefore, we have come to convince ourselves that laser trapping will make it possible to crystallize molecules in solution by stimulating the gathered assembly. Namely, laser-trapping crystallization was explored as one of interesting and fruitful laser chemistry and actually we succeeded in demonstrating it in 2007 [9].

In the history of crystal chemistry the role of light has been a tool for characterizing crystals and for providing their functions, while light-induced crystallization was reported in 1996 [10]. Garetz and Myerson showed that irradiation of nanosecond laser pulse into supersaturated solution of urea and amino acids results in their crystallization. They also successfully controlled crystal polymorph in glycine and histidine crystallization [11,12]. Their interpretation was based on re-orientation of molecules in supersaturated solution triggering alignment favorable to crystals, and they are developing their studies along this line. This nanosecond laser-induced crystallization was recently reported also for inorganic crystal, and pulse width effects on the crystallization were discussed [13–15]. In 2002, we first demonstrated femtosecond laser-induced crystallization of lysozyme and are still confirming the dynamics and mechanism [16]. The multiphoton absorption led to solution ablation, accompanied with bubble generation, above a certain threshold of laser power. The produced concentration inhomogeneity may trigger the nucleation where the interface between the bubble and solution has an important role. Tashiro et al. reported a similar result [17], while our method has been extended to more complex proteins by Adachi, Mori, Sasaki et al. [18]. As a photochemical approach, Okutsu excited tryptophan in lysozyme and induced dimerization. The formed lysozyme dimer has less solubility, so that it becomes a nice impurity for generating lysozyme crystal [19]. It should be described that prepared crystal structure is better than that by conventional crystallization methods and efficiency is much enhanced.

Laser trapping may be another possible way of laser-induced crystallization. Actually, laser trapping of amino acids and attempts of crystallization for some proteins were demonstrated by Tsuboi and Kitamura [20], but only assembling giving a microparticle was observed and no crystallization was completed. We understand that their experiment was conducted in solution and just gathering at the focal point was not enough to prepare crystals. In 2007, we were lucky to have a chance to generate a single crystal just by trapping glycine clusters in solution [9]. Later, by examining the conditions we understand that the irradiation at a solution surface is critical. Namely, the creation of a highly concentrated region by laser trapping and some alignment at the surface layer are both necessary for generating crystals. Actually, not only supersaturated but also unsaturated solution of glycine underwent crystallization by laser trapping [21], while no crystal formation was observed but the millimeter-sized giant

droplet was prepared when the laser beam was focused at an interface between solution and glass substrate [22]. At the present stage of investigation, the following knowledge is obtained. Heavy water is used, as its absorption at 1064 nm is smaller than that of H_2O, suppressing local heating effect. Crystal polymorph, namely, α- or γ-form of glycine, can be controlled by laser power and polarization. In unsaturated solution, crystallization time becomes longer and the prepared crystal disappears soon; namely, a repeated behavior of crystallization and dissolution is observed.

Now we are devoting our efforts to make clear experimental conditions, to explore protein crystallization, and to reveal the dynamics and mechanism of laser-trapping assembling and crystallization processes. In this article, some of the results which we have obtained recently are presented and compared with those mentioned above. First, laser-trapping crystallization of glycine in H_2O is shown and the difference between D_2O and H_2O is considered. Second, droplet formation of urea upon laser irradiation at an interface between solution and glass is summarized and the comparison with glycine is made. Third, a new trial of laser-trapping assembling and precipitation of supramolecular protein is reported. Finally, we summarize the present status of laser-trapping crystallization study and describe our perspective.

LASER-TRAPPING CRYSTALLIZATION OF GLYCINE IN H_2O

Glycine has been widely employed as a representative model compound for studying crystallization dynamics and mechanism, and three polymorphs of α, β, and γ are well known where their thermodynamic free energy is in the order of γ (most stable) < α < β (least stable) [23–28]. α-Form is always given by conventional crystallization methods, indicating that this form is kinetically most probable among the three forms [29]. The least stable β-form is prepared in the mixture of water and ethanol, but it is rapidly transformed into the α-form in air or water [30,31]. This behavior is consistent with the fact that both crystal structures are much similar to each other and the β-form is regarded as a quasi-stable state of the α-form. The γ-form is generated only when high pressure is applied, the evaporation rate is controlled to be considerably slow, or high acidic/basic aqueous solution is used [27,29,32–36]. This means that thermodynamically favored but kinetically slow crystallization process to γ-form is accelerated, overcoming the process to the α-form, under such unconventional conditions. These conditions are considered to give eventually high supersaturation degree, where crystallization is controlled just thermodynamically, namely, the γ-form is selected. One more advantage of glycine for laser-trapping crystallization study is that this compound is known to form a liquid-like cluster in highly concentrated solution [37]. This cluster contains water molecules, its size reaches to a few tens of nanometers, and its polarizability is higher than that of water. These characteristics enable us to trap the liquid-like cluster in an optically prepared potential well. Namely, the clusters can be gathered and new phenomena can be realized by focusing the intense CW 1064-nm beam.

We succeeded for the first time in demonstrating laser-trapping crystallization of glycine in D_2O and are extending systematically this study [9,21,22,38]. The superiority of this crystallization method is summarized as follows: (1) One single crystal is always prepared at the focal point, where the crystal is kept upon irradiation. Namely, we can fabricate one single crystal in temporally and spatially controlled manner. (2) Crystal polymorph can be controlled by changing laser power and polarization. (3) Irradiation at the air/solution interface is necessary for generating a crystal, and no crystallization was observed upon irradiation in the solution or at the glass/solution interface. (4) D_2O is a favorable solvent instead of H_2O, as the latter absorbs 1064-nm photons through overtone vibration of O–H bonds leading to temperature elevation. Actually, Ito et al. estimated the temperature elevation at the focal spot in H_2O and D_2O by applying fluorescence correlation spectroscopy to 22–24 and 2.0 *K*/W, respectively [39]. The temperature change is, of course, critical as solubility is much affected. Until now we have studied the trapping crystallization of glycine in D_2O, while it is necessary to investigate what happens in H_2O and to compare the dynamics to that in D_2O, which is reported here.

Glycine (>99 % pure) and H_2O (>99.9 % pure) were used without any purification. The saturated solution of glycine used in this experiment was prepared as follows; 0.23 g of glycine was dissolved in 1.0 g of H_2O while keeping at 60 °C and shaking for 3 h, and the solution was slowly cooled down to room temperature, at which it then aged statically for 1 day. A 15-μL of the saturated solution was dropped into a hand-made sample bottle with a highly hydrophilic bottom surface, the portion immediately spread all over the cover glass, and the solution thin film with a thickness of about 120 μm was spontaneously formed. Then, the bottle was immediately and completely sealed with a spigot to suppress solvent evaporation, and was put on the stage of an inverted microscope. The laser-trapping system was almost the same as described in the reference [38]. A linearly polarized 1064-nm laser beam was introduced into an inverted microscope and focused at the air/solution interface of the solution layer. The laser power throughout the objective lens was varied from 0.8 to 1.4 W by tuning a half-wave plate coupled with a polarizing beam splitter. Crossed Nicols images were recorded during the crystallization by an electron-multiplied charge-coupled device (EMCCD) video camera.

The laser-trapping crystallization was achieved also in H_2O, and their representative CCD images are shown in Fig. 1. At 30 s after focusing the laser beam at the air/solution interface, a liquid-like domain was clearly confirmed as in Fig. 1a. This domain was not kept stably at the focal spot and floated away soon. It is interesting to see that the domain grew continuously from the focal spot, which was something like a fountain. This floating phenomenon has never been observed in D_2O, where the crystal was formed and trapped. We consider that this phenomenon is due to vigorous convection flow, which is ascribed to local temperature elevation characteristic of H_2O irradiated by the 1064-nm beam. When the growing and floating away of the domain was accidentally stopped with the laser on, the domain was immediately changed to a crystal with sharp edges as shown in Fig. 1b. This is the crystallization behavior of glycine in H_2O. We repeated this experiment 10 times at each laser power and always observed the same behavior.

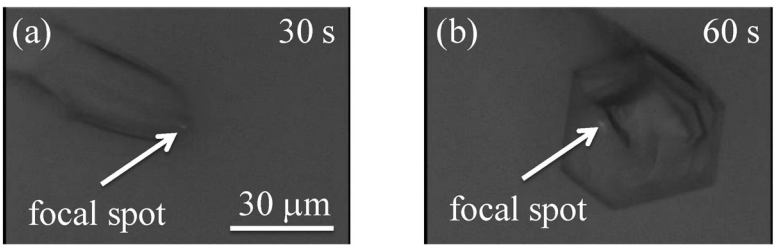

Fig. 1 CCD images of crystallization behavior of glycine in H_2O solution during laser irradiation.

In relation to the domain formation, we point out the relation to the millimeter-sized liquid droplet formation in D_2O solutions of glycine [22,40]. The formation is observed clearly only when the laser beam is focused at the glass/solution interface, and is considered to be brought about by efficient assembling of liquid-like clusters. Upon switching off the laser beam, the droplet disappears in a few tens of seconds and never undergoes to crystallization. We interpret the droplet formation in terms of liquid/liquid phase separation due to local concentration increase, which is supported by direct measurement of refractive index change. Temperature elevation should not be a main reason, as D_2O does not absorb the trapping laser beam and temperature elevation is estimated to be less than one-tenth compared to in H_2O. On the other hand, the domain in H_2O was changed immediately to the crystal. The solubility of glycine in H_2O and D_2O is almost same [41], so that the transformation to each domain possibly occurs at the same concentration. The domain formation in H_2O requires the higher concentration compared with that in D_2O because of higher-temperature elevation given at the same power. Upon stopping the flow of the formed domain, it steadily occupied the focal spot, where temperature elevation due to laser

irradiation is suppressed, leading to the increase in concentration. Thus, one possible explanation of this novel behavior is that the higher increase in concentration in H_2O triggers the rapid crystallization.

The domain formation time in H_2O is comparable to crystallization time in D_2O, and high-temperature elevation in H_2O is expected to slow down the formation rate of the domain. Actually, the domain growing rate became slow with time. This result strongly supports an idea that laser trapping of the liquid-like clusters competes with dissolution carried out by temperature elevation as supersaturation degree decreases with increase in temperature. The higher saturation degree at higher temperature prohibits crystallization, giving such a domain.

The polymorph of the formed crystal was characterized by Fourier transform-infrared (FT-IR) measurement, while we confirmed that the characterization by FT-IR measurement is in good agreement with that by X-ray crystallographic analysis of the single crystal except for β-glycine [38], which was assigned only by the FT-IR measurement on the basis of the reported data [42]. In this experiment, a saturated solution was used as an initial solution so that the concentration after the trapping crystallization should be lower than the saturation degree. Therefore, immediately after the laser-trapping crystallization, the spigot was opened in order to make the crystal large. After picking the large crystal, FT-IR measurement was performed. We found that all of the obtained spectra were classified into three types as shown in Fig. 2, and no mixture of them was confirmed. Namely, one single crystal is always given, which suggests that crystallization develops from a single nucleus. All their vibrational absorption peaks agree well with those of three polymorphs of α, β, and γ reported previously [43–45]. It is worth noting, particularly from viewpoints of polymorph control, that the crystal form depends on the laser power, which result is summarized in Table 1. In general, α-glycine is prepared by conventional methods, but laser trapping at 1.1 and 1.2 W now gives the β-form, which is the least stable, although its probability is about 10 %. Laser-trapping crystallization in D_2O did not give the β-form. It is known that β-glycine is gradually transformed into α-one in air, but no transformation occurs during the growth. Indeed, a crystal, which was characterized as the β-form by FT-IR measurement just after picking it up from the solution, changed into the α-form in 30 min, and after 2 days the mixture of α- and γ-forms was identified. Such transformation of glycine crystal under ambient conditions has been investigated in detail [46], and our results are consistent with the report. Anyway, it is worth noting that the unconventional and non-stable β-glycine crystal can be obtained by laser-trapping method and that not only laser power but also solvent are determining parameters of the crystal polymorph. In the conventional crystallization, this β-form is prepared when ethanol or acetic acid is added to water, and this

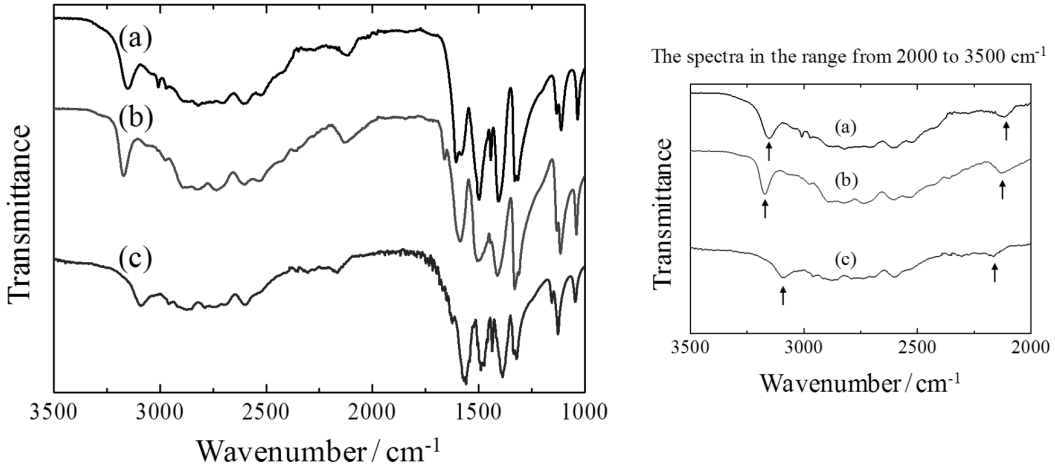

Fig. 2 FT-IR spectra of glycine crystals prepared by laser trapping in H_2O solution with a focused CW NIR laser beam. Obtained spectra are assigned to α- (a), β- (b) and γ-forms (c) of glycine, respectively.

behavior is considered to be due to the change of the hydrogen-bonding network involving carboxyl and amino groups of glycine molecules [47,48]. The present experiment was performed by focusing the trapping beam at the air/solution interface, so that mutual orientation and alignment of glycine molecules in the layer are more flexible than in the bulk and much affected by the intense light field of the trapping beam. Thus, although the whole mechanism has not been cleared yet, we consider that the crystal polymorph can be determined by a nice coupling among laser power, polarization, saturation degree, solvent, temperature, and diffusion near the surface. It can be said that laser-trapping crystallization is opening a new horizon in molecular crystallization studies.

Table 1 Crystal polymorph of glycine crystal formed by laser-trapping crystallization in H_2O solution.

Laser power (W)	α-form (%)	β-form (%)	γ-form (%)
0.8	85	0	15
1.0	85	0	15
1.1	89	11	0
1.2	90	10	0
1.4	100	0	0

LASER-TRAPPING DROPLET FORMATION OF UREA IN D_2O

As introduced above, the irradiation position is very critical to achieve laser-trapping crystallization, and glycine in D_2O gave a millimeter-sized droplet upon irradiation at the glass/solution interface. In order to confirm whether this unique behavior is just for glycine or general and to elucidate its formation mechanism, it would be requested to examine other compounds. Here, urea is selected as we reported already femtosecond laser-induced crystallization and crystal growth of urea [49]. Its solubility curve in water is quite different from that of glycine and has a sharper change in temperature, so that urea will be a nice reference for considering relations between droplet formation and crystallization.

Urea solutions with 28 and 136 % saturation values were prepared by dissolving 0.30 and 1.43 g of commercial urea (>99.0 % pure) in 1.0 g of D_2O (99.9 % pure), respectively. These solutions were kept at 40 °C with vigorous shaking for 3 h, followed by slow cooling down to room temperature. A 40-μL portion of the solution was put on a cover glass with a highly hydrophilic surface, which was immediately covered with a petri dish, for the suppression of solvent evaporation, and the solution layer was formed. The experimental set-up used for the laser-trapping experiment is the same as that reported [22], where a laser confocal displacement meter was placed above the sample stage of the inverted microscope. Thus, it was possible to measure the temporal change of the solution surface height during laser irradiation. The surrounding area at the focal spot was observed by naked eye and a CCD camera.

Upon focusing the trapping laser of 1064 nm with 1.1 W at the glass/solution interface, we found formation of a single millimeter-sized liquid droplet in the solution film as shown in Fig. 3a. Before laser irradiation, only a cover glass and the top of an objective lens were observed, while after irradiation, the formation of the single millimeter droplet was clearly and directly observed. This result on the D_2O solution of urea is similar to that of D_2O solution of glycine [22]. This behavior was followed quantitatively as temporal change of the surface height at the focal axis. The growing of the droplet and the corresponding surface height change are shown in Figs. 3b,c, respectively. Initial surface height, that is the thickness of the solution film, was 120 μm. At that time, only the top of the objective lens was identified as a dark disk through the solution in Fig. 3b (1). After starting irradiation, the surface height monotonously decreased and went down to about 5 μm in 20 s. Here, as shown in (2) of Fig. 3b, no apparent change in the CCD image was observed. Such surface depression has been reported and explained on the basis of inhomogeneous distribution of surface tension induced by local temperature elevation [50,51]. Further laser irradiation induced the continuous surface elevation, and a spheri-

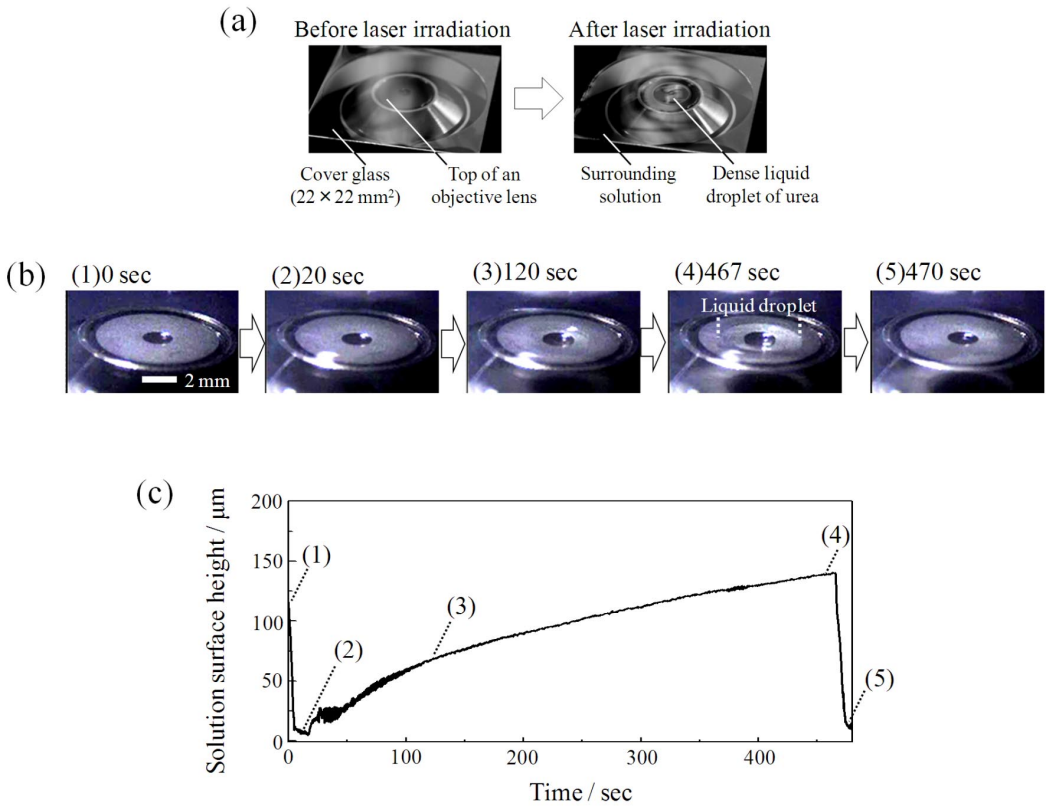

Fig. 3 (a) Photographs of urea unsaturated D_2O solution (28 %) before and after laser irradiation. (b) A series of CCD images around a focal spot during the irradiation. (c) Temporal change of surface height in urea unsaturated solution during laser irradiation. Each image of (1)–(5) in (a) corresponds to (1)–(5) in (b), respectively. Time is defined as $t = 0$ on turning on laser beam.

cal droplet became clearly visible around the focal spot as shown in (3) of Figs. 3b,c. At about 470 s, the droplet eventually grew to the size of 4.6 mm in diameter and 140 μm in height, as could be seen even by the naked eye in Fig. 3b (4). Then, the droplet suddenly disappeared and the height decreased to 10 μm in (5) of Figs. 3b,c. This disappearance was repeatedly observed for 5 samples, and occurred at the height ranged from 110 to 150 μm. Again, the present behavior confirmed for 28 % solution is quite similar to that of glycine reported previously [22].

In order to characterize the urea droplet in the 28 % solution, we measured the refractive index change by backscattering using a He–Ne laser and confirmed that the droplet has higher molecular concentration compared with the initial solution. Another important result is that its size is much larger than the focal spot of about 1 μm. Since these features of the droplet are quite similar to that in a glycine solution reported previously [22], we suggest that this droplet formation is possibly triggered by the liquid/liquid phase separation due to laser trapping of the liquid-like clusters. Experimentally, glycine liquid-like clusters consisting of the dimers under supersaturated conditions have been confirmed by small-angle X-ray scattering (SAXS) measurement [37], while the object size we can trap in the present laser power of 1.1 W is approximately calculated to be above 17 nm. Thus, it should be assumed that urea forms liquid-like clusters with the size of this order.

Myerson et al. reported that the diffusion coefficient of urea molecules in water drastically decreases at the saturation concentration, and pointed out that the aggregations or clusters of the molecules may be formed under supersaturated conditions [52]. However, in the dilute solution used in this

experiment, the presence of such clusters is less likely. The monomers should exist in the solution, and they are too small to be trapped. Here, we remember that the laser beam was focused into the deformed solution during irradiation. It is worth noting that Louchev et al. theoretically revealed that molecules dissolved in solution are efficiently supplied into the surface depression area, where photon pressure acts, due to mass transfer by Marangoni convection [53]. As a result, the transfer is enhanced by a magnitude of one to two orders. Therefore, we suggest that a focused laser beam induces the increase of molecular concentration around the focal spot, possibly leading to the cluster formation and its efficient trapping. Actually, the droplet formation occurred always after the surface depressed to a few μm height. In the process of spontaneous growth after the nucleation, the dense droplet preferred a sphere shape because of the high surface energy. As a result, the surface height increased almost to the initial position in Fig. 3c. We suggest that further droplet growth should generate larger inhomogeneous distribution of the surface energy. Thus, the droplet disappeared at a certain height in order to cancel the imbalance of surface tension between the droplet and surrounding solution.

On the other hand, no droplet formation was observed for the 136 % solution. Figure 4 shows the temporal change of the surface height during laser irradiation. Only slight surface depression of about 10 μm was observed, and direct CCD observation showed no change. After the depression, the surface recovered almost to the initial position, and further irradiation induced no more surface change. In neat D_2O, the droplet formation is never seen, but evaporation at the focal spot was completed as shown in Fig. 5. The oscillation observed from 8 to 20 s is possibly ascribed to some kinds of standing wave at the surface.

The contrastive results on urea solutions of 28 and 136 % saturation cannot be explained only in view of temperature elevation, which is carried out by absorption of 1064-nm photons through urea vibrational overtone bands. No large surface depression was observed in the supersaturated solution, although temperature elevation results in surface morphological change. Here, we should note the fact that such solution deformation and convection are induced only when temperature gradient across a liquid layer becomes large enough to overcome the resistances of viscosity and thermal diffusivity [51]. The viscosity of the supersaturated solution is calculated to be about two times higher than that of the unsaturated one [54], so that the higher viscosity inhibits the large solution deformation. Furthermore, mass transfer due to convection also accelerates the heat diffusion. As a result, the temperature distribution close to the solution surface should become uniform within a short time, leading to the quick recovery to the initial height as shown in Fig. 4. Thus, these results strongly support that the surface depression to a few μm height plays an important role for forming the dense liquid droplet.

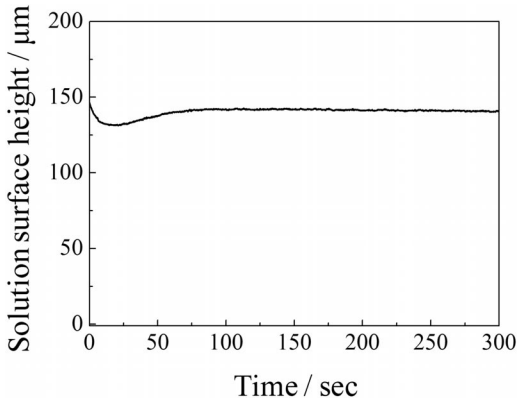

Fig. 4 Temporal change of the surface height of supersaturated D_2O solution of urea (136 %) upon focusing the laser beam at a glass/solution interface.

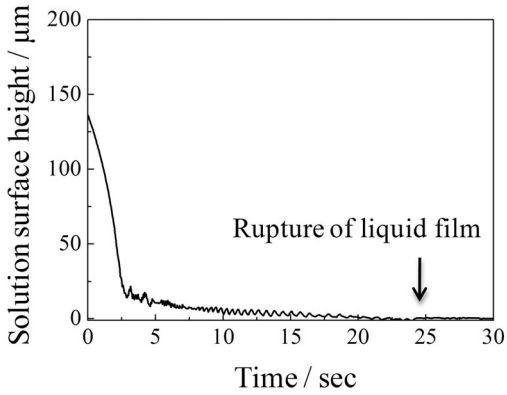

Fig. 5 Temporal change of the surface height of neat D_2O upon focusing the laser beam at a glass/liquid interface.

LASER-TRAPPING ASSEMBLY AND PRECIPITATION OF SUPRAMOLECULAR PROTEIN IN D_2O

One of the key issues for laser-trapping crystallization is whether or not this phenomenon can be induced for proteins and their single crystals can be obtained. Here we report our examinations on the laser-trapping assembling of a giant supramolecular protein: ferritin. The spherical hollow shell (13 and 7 nm of outer and inner diameter) is composed of 24 subunits (~450 kDa) and accommodates ferrihydrite nanoparticle in its cage in nature [55,56]. Ferritin is highly symmetric and possesses high structural strength and thermo-tolerance [57]. The ferritin size is large enough for laser trapping, and we consider that its intrinsic symmetry and structural stability are suitable for the formation of well-ordered molecular assembly structure under laser trapping. Actually, we have succeeded in observing huge and rapid molecular assembly formation of cobalt oxide nanoparticle-accommodated ferritin by laser trapping at the solution surface. It grew to the size larger than that of the trapping laser spot. We also found that the laser trapping-induced assembling behavior of ferritin strongly depended on the laser focal position; at the air/solution interface, inside of the solution, or at the glass/solution interface.

A recombinant deletion mutant ferritin (Fer8) which lacks eight *N*-terminus amino acids of L-chain apoferritin was used. Details of expression, over-production and purification of apoferritins were described elsewhere [58–60]. Artificially biomineralized Co_3O_4 nanoparticles in Fer8 cavity were prepared with one-pot synthesis [61]. Hereafter the nanoparticle-accommodated Fer8 is called Co-Fer8, whose schematic representation is shown in Fig. 6. The concentration of sample solutions was adjusted to 0.5~5.0 mg/mL in D_2O. Prepared ferritin solutions were filtered to remove aggregated molecules

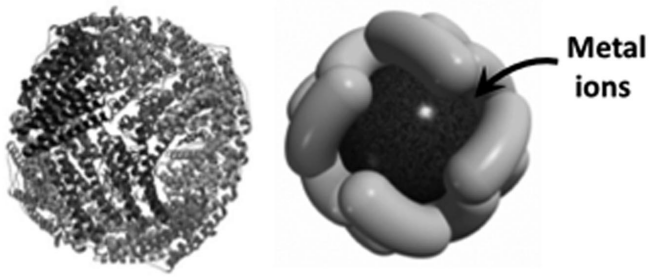

Fig. 6 Illustrations of a ribbon model of Fer8 (left) and cross-sectional view with schematically depicted subunits and biomineralized nanoparticles in protein cage (right). Both are viewed from the four-fold axis. Metal ions are introduced from a three-fold channel. Ferritin has 13- and 7-nm outer and inner diameter, respectively.

prior to the use. It should be noted that the sample solutions were not supersaturated and never showed precipitation due to aggregation of protein molecules for more than 2 weeks. Typically, 20 μL of Co-Fer8 solution was put on a cleaned glass substrate equipped with an air-tight sample chamber to prevent rapid solvent evaporation. The thickness of the solution thin film was typically around 100 μm. Linearly polarized near-infrared CW laser beam (λ = 1064 nm) of 0.1–1.4 W was focused to the surface/interface or in the solution.

By focusing the trapping laser to the sample solution, we observed the formation of Co-Fer8 assembly structure. Interestingly, the shape of the formed assembly structure changed depending upon the irradiation position. Microscope images depicted in Fig. 7 show representative wire- and disk-shaped assembly upon focusing to the air/solution interface (Fig. 7a) and in the solution (Fig. 7b), respectively. We should note that these assembly formations could be achieved only by irradiating the focused laser, and simple evaporation of solution never gave such exotic assembly structures.

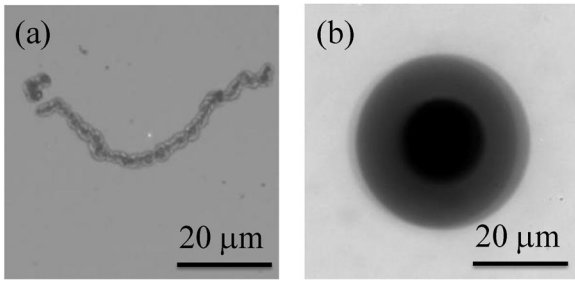

Fig. 7 Optical transmission images of Co-Fer8 assemblies fabricated by focusing the trapping laser to the air/solution interface (a) and in the D_2O solution (b). Co-Fer8 concentration and trapping laser power was 5 mg/mL and 200 mW, respectively.

Figure 8 shows the pictures taken during the wire-assembly formation by focusing the 500-mW trapping laser to the air/solution interface of 2 mg/mL Co-Fer8 solution. We could not find any assembly immediately after starting irradiation (Fig. 8a). At 3.5 s later, a small spherical assembly, which size is 1.5 μm in diameter, suddenly appeared in CCD image (Fig. 8b). Continuous laser trapping of it induced its growth and it changed into the wire-like form, as seen in Figs. 8c,d, at 5 and 8 s later after starting the laser trapping. The length of the wire became 17.5 and 33.3 μm, in Figs. 8c,d, respectively. The assembly formation rate was quite fast and took only 4.5 s to form a 33.3-μm wire-shaped molecular assembly of protein. As we can see in Fig. 8, the wire seemed to be formed by linking the small spherical particles, which suggests that very rapid successive formation of spherical particle formation occurred under laser trapping and formed particles were connected. The wire assembly formed was insoluble even after turn-off of the trapping laser.

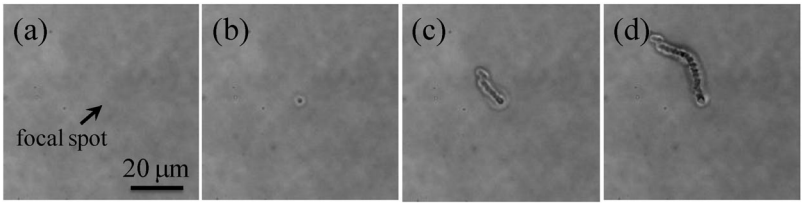

Fig. 8 Sequential pictures taken during laser trapping of Co-Fer8 by focusing the laser at the air/solution interface. Images are taken at (a) 0.5 s, (b) 3.5 s, (c) 5 s, and (d) 8 s after starting trapping laser irradiation. Co-Fer8 concentration: 2 mg/mL. Trapping laser power: 500 mW. An arrow indicates the position of trapping laser spot.

Conversely, we observed the big 2D disk-like assembly for apoferritin, i.e., ferritin without nanoparticle formation, by focusing the trapping laser at the air/solution interface. However, the assembling behavior observed in Co-Fer8 was obviously different from that of apoferritin at some points. First, the laser power and protein concentration of Co-Fer8 were not extreme as for apoferritin. It was also confirmed that the assembling rate was quite different. Co-Fer8 was assembled within a few to a few tens seconds under 1 W laser, ~5 mg/mL protein concentration at the air/solution interface. A typical assembly formation of 2D-disk of apoferritin needed more than 10 min under the same conditions of concentration and laser power. Figure 9 summarizes the necessary laser power to induce the assembly formation at various solution concentrations. The threshold of assembly formation was much lower than that for apoferritin (5 mg/mL and >1 W). Surprisingly, the necessary concentration is lower and laser power can be decreased to one order of magnitude smaller (100 mW). Second, we could induce the big assembly formation even in the solution only for Co-Fer8 and never for apoferritin. The size of the Co-Fer8 protein assembly reached larger than 10 μm in most cases, and its structure was different from that of apoferritin. Furthermore, the formed Co-Fer8 assembly could be conserved after the turn-off of the trapping light, while apoferritin gave only a tentative huge 2D disk assembly and the structure will vanish by shutting down the trapping laser beam.

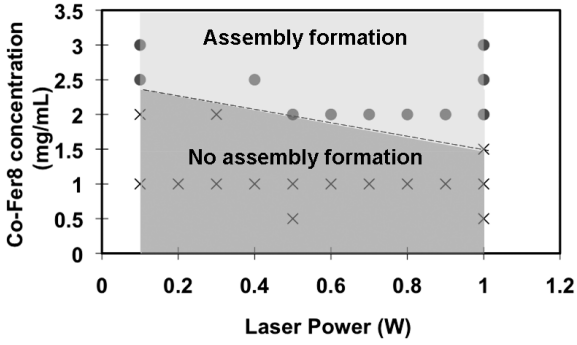

Fig. 9 Trapping laser power and concentration dependence of Co-Fer8 assembly formation by focusing the trapping laser at the air/solution interface. Filled circle and cross mark indicate successful assembly formation and failure on assembly formation, respectively. Dashed line in the figure indicates suggests threshold for the assembly formation.

Assembly and precipitation of proteins are realized for Co-Fer8, while one of the authors has reported the laser trapping-induced assembly formation for a polymer molecule [62,63]. The former case is achieved upon irradiation at the air/solution interface and not in solution. As described above, crystallization is realized only at the air/solution surface, where molecular assembly formation is induced due to laser trapping of the clusters. In the case of polymers, crystallization is not induced, which is consistent with polymer characteristic, and the wire-type assembly is prepared. On the contrary, the formation of Co-Fer8 is achieved not only at the surface but also inside the solution, so that laser trapping of Co-Fer8 is very unique and hopefully a new approach to fabricate biomolecular assemblies. Furthermore, the assembly size and fabrication position can be controlled by adjusting irradiation conditions, and addition of functional groups for specific recognition enables a deposition and patterning to solid substrate.

As a plausible explanation for the present phenomenon of Co-Fer8, we consider that relatively high refractive index of cobalt oxide nanoparticle enhanced the trapping efficiency. The real part of the refractive index of Co_3O_4 at 1 μm was reported as ~2.1 [64], which is much higher than that of ferritin (~1.45) [65]. As a result, Co_3O_4 has weak absorption in the near-infrared region [66], so that we can expect resonance effect on laser trapping [67,68], and simultaneously should take temperature elevation

due to the light absorption into account. The resonance effect means that the laser-trapping force is enhanced very much when electronic transition energy of the target is resonated with the trapping laser itself and/or additional laser. This effect was experimentally demonstrated in our previous report [68]. As we mentioned above, we observed very fast assembly formation with low laser power even in the solution only on Co-Fer8 case. We consider that it can be explained by the resonance enhancement due to weak absorption of Co_3O_4 at trapping laser wavelength.

In addition to the resonance effect, photothermal temperature elevation should be involved. It may lead to a denaturation of ferritins and deformation of Co_3O_4 nanoparticles. Cobalt metal ions and the nanoparticles kicked out from ferritin cage will enhance the association of Co-Fer8s, giving nanostructures. This trapping and decomposable association are coupled with solvent flow at the air/solution interface and diffusion in the surface layer, which will be an origin of the wire-shaped structure. In view of high thermal resistivity of ferritin (~90 °C), thermal denaturation of protein is not so easy under conventional laser trapping in water, but without hydrophobic interaction due to the hydrophobic internal surface of Co-Fer8 exposed by denaturation, the stable wire-like assembly could not be realized. Of course, thermal effect is an unavoidable issue for the use of biological molecule, and spectroscopic observations of the temperature elevation at and surroundings of the laser spot and structural characterization of formed assembly under microscope are necessary, but still it is worth noting that laser trapping and precipitation is demonstrated for supramolecular protein.

SUMMARY AND PERSPECTIVE

Laser trapping has been recognized as a useful tool for manipulating micrometer-sized small objects and has received much attention in bioscience and biomedical technology. Isolated molecules are usually too small to be trapped in solution at room temperature, but when they form clusters and associate with each other, giving supramolecular structures, it should be possible. Even the molecular concentration is low to form clusters, trapping at the focal point assists clustering, and molecules are transported from outside by laser-induced convection, resulting in the laser trapping.

In the case of glycine in H_2O, crystallization dynamics was confirmed to be different from that in D_2O, which is ascribed to heating effect due to the absorption of 1064-nm light through an overtone vibrational band of H_2O. A very unconventional polymorph of β-form crystal was successfully prepared, although its probability is ~10 %. When an unsaturated D_2O solution of urea was irradiated at the glass/solution interface, a single giant droplet was formed, leading to a large change in solution height. This formation behavior shows concentration dependence, which is interpreted in terms of intermolecular hydrogen-bonding interaction and molecular diffusion. Metal nanoparticle-accommodated ferritin could be trapped with low laser power, suggesting resonance effect in laser trapping. Its laser trapping leads to precipitation of wire-shaped structures, and it is stable even after switching off the laser beam.

All these phenomena are started by laser trapping at the focal point and completed by forming a few tens micrometer-to-millimeter-sized products. The initial orientation and association of molecules at the focal volume extended and grew to outside, which is based on intermolecular interactions and coupled with diffusion, thermal conduction, and/or deformation of solution film. It is considered that nucleation is a key step for crystallization, liquid/liquid phase separation, and precipitation.

We plan to explore further new molecular phenomena induced by laser trapping and to confirm that the behavior is general. Until now, most of the spectroscopic analyses of laser trapping were done in the focal point, but we point out that the simultaneous dynamic diffusion analysis and spatio-temporal measurement outside the focal volume are necessary and indispensable for understanding the nature of the relevant phenomena. As a first step, we are developing wide-field Rayleigh scattering spectroscopic imaging and applying it to gold nanoparticle systems.

ACKNOWLEDGMENTS

The present work is partly supported by a KAKENHI (S) grant (a Grant-in-Aid for Scientific Research) (No. 18106002) from the Japan Society for the Promotion of Science (JSPS) to H.M., the MOE-ATU Project (National Chiao Tung University) of the Ministry of Education, Taiwan, to H.M., the National Science Council of Taiwan (No. 0970027441) to H.M., a KAKENHI grant on Priority Areas "Strong Photon-Molecule Coupling Fields (Area No. 470)" from the Ministry of Education, Culture, Sports, Science and Technology of Japan (MEXT) (No. 21020022) to T.S., and a KAKENHI (C) grant (No. 20550136) to T.S.

REFERENCES

1. H. Masuhara. *Pure Appl. Chem.* **64**, 1279 (1992).
2. H. Masuhara. *J. Photochem. Photobiol. A* **62**, 397 (1992).
3. H. Masuhara, N. Kitamura, H. Misawa, K. Sasaki, M. Koshioka. *J. Photochem. Photobiol. A* **65**, 235 (1992).
4. H. Masuhara, F. C. De Schryver, N. Kitamura, N. Tamai (Eds.). *Microchemistry: Spectroscopy and Chemistry in Small Domains*, North Holland/Elsevier (1994).
5. H. Masuhara, T. Asahi, Y. Hosokawa. *Pure Appl. Chem.* **78**, 2205 (2006).
6. H. Masuhara, F. C. De Schryver (Eds.). *Organic Mesoscopic Chemistry* (IUPAC 21st century chemistry monograph), Blackwell Science, Oxford (1999).
7. H. Masuhara, H. Nakanishi, K. Sasaki (Eds.). *Single Organic Nanoparticles*, Springer, Berlin (2003).
8. H. Fukumura, M. Irie, Y. Iwasawa, H. Masuhara, K. Uosaki (Eds.). *Molecular Nano Dynamics*, Vols. 1 and 2, Wiley-VCH (2008).
9. T. Sugiyama, T. Adachi, H. Masuhara. *Chem. Lett.* **36**, 1480 (2010).
10. B. A. Garetz, J. E. Aber, N. L. Goddard, R. G. Young, A. S. Myerson. *Phys. Rev. Lett.* **77**, 3475 (1996).
11. X. Sun, B. A. Garetz, A. S. Myerson. *Cryst. Growth. Des.* **6**, 684 (2006).
12. X. Sun, B. A. Garetz, A. S. Myerson. *Cryst. Growth. Des.* **8**, 1720 (2008).
13. A. J. Alexander, P. J. Camp. *Cryst. Growth. Des.* **9**, 958 (2009).
14. M. R. Ward, I. Ballingall, M. L. Costen, K. G. McKendrik, A. J. Alexander. *Chem. Phys. Lett.* **481**, 25 (2009).
15. C. Duffus, P. J. Camp, A. J. Alexander. *J. Am. Chem. Soc.* **131**, 11676 (2009).
16. H. Adachi, Y. Hosokawa, K. Takano, F. Tsunesada, H. Masuhara, M. Yoshimura, Y. Mori, T. Sasaki. *J. Jpn. Assoc. Cryst. Growth* **29**, 445 (2002).
17. S. Watanabe, S. Nagasaka, K. Noda, H. Tashiro. *J. Jpn. Appl. Phys.* **43**, L941 (2004).
18. H. Adachi, S. Murakami, A. Niino, H. Matsumura, K. Takano, T. Inoue, Y. Mori, A. Yamaguchi, T. Sasaki. *J. Jpn. Appl. Phys.* **43**, L1376 (2004).
19. T. Okutsu. *J. Photochem. Photobiol. C: Photochem. Rev.* **8**, 143 (2007).
20. Y. Tsuboi, T. Shoji, N. Kitamura. *J. Phys. Chem. C* **114**, 5589 (2009).
21. T. Rungsimanon, K. Yuyama, T. Sugiyama, H. Masuhara. *Cryst. Growth Des.* **10**, 4686 (2010).
22. K. Yuyama, T. Sugiyama, H. Masuhara. *J. Phys. Chem. Lett.* **1**, 1321 (2010).
23. K. Srinivasan. *J. Cryst. Growth* **311**, 156 (2008).
24. E. V. Boldyreva, V. A. Drebushchak, T. N. Drebushchak, I. E. Paukov, Y. A. Kovalevskaya, E. S. Shutova. *J. Therm. Anal. Cal.* **73**, 409 (2003).
25. E. V. Boldyreva, V. A. Drebushchak, T. N. Drebushchak, I. E. Paukov, Y. A. Kovalevskaya, E. S. Shutova. *J. Therm. Anal. Cal.* **73**, 419 (2003).
26. G. L. Perlovich, L. K. Hansen, A. Bauer-Brandl. *J. Therm. Anal. Cal.* **66**, 699 (2001).
27. Y. Itaka. *Acta Crystallogr.* **14**, 1 (1961).

28. G. Albrecht, R. B. Corey. *J. Am. Chem. Soc.* **61**, 1087 (1939).
29. K. Srinivasan. *J. Cryst. Growth* **311**, 156 (2008).
30. I. Weissbuch, V. Y. Torbeev, L. Leiserowitz, M. Lahav. *Angew. Chem., Int. Ed.* **44**, 3226 (2005).
31. E. S. Ferrari, R. J. Davey, W. I. Cross, A. L. Gillon, C. S. Towler. *Cryst. Growth. Des.* **3**, 53 (2003).
32. X. Yang, J. Lu, X. J. Wang, C. B. Ching. *J. Cryst. Growth* **310**, 604 (2008).
33. T. Balakrishnan, R. R. Babu, K. Ramamurthi. *Spectrochim. Acta A* **69**, 1114 (2008).
34. M. N. Bhat, S. M. Dharmaprakash. *J. Cryst. Growth* **242**, 245 (2002).
35. G. He, V. Bhamidi, S. R. Wilson, R. B. H. Tan, P. J. A. Kenis, C. F. Zukoski. *Cryst. Growth Des.* **6**, 1746 (2006).
36. A. Dawson, D. R. Allan, S. A. Belmonte, S. J. Clark, W. I. F. David, P. A. McGregor, S. Parsons, C. R. Pulham, L. Sawyer. *Cryst. Growth Des.* **5**, 1415 (2005).
37. S. Chattopadhyay, D. Erdermir, J. M. B. Evans, J. Ilavsky, H. Amentisch, C. U. Segre, A. S. Myerson. *Cryst. Growth Des.* **5**, 523 (2005).
38. T. Rungsimanon, K. Yuyama, T. Sugiyama, H. Masuhara, N. Tohnai, M. Miyata. *J. Phys. Chem. Lett.* **1**, 599 (2010).
39. S. Ito, T. Sugiyama, N. Toitani, G. Katayama, H. Miyasaka. *J. Phys. Chem. B* **111**, 2365 (2007).
40. K. Yuyama, K. Ishiguro, T. Rungsimanon, T. Sugiyama, H. Masuhara. *Proc. SPIE* **7762**, 776236 (2010).
41. K. S. Kunihisa. *J. Cryst. Growth* **23**, 351 (1974).
42. G. B. Chernobai, Y. A. Chesalov, E. B. Burgina, T. N. Drebushchak, E. B. Bokdyreva. *J. Struct. Chem.* **48**, 332 (2007).
43. L. Stievano, F. Tielens, I. Lopes, N. Folliet, C. Gervais, D. Costa, J. F. Lambert. *Cryst. Growth Des.* **10**, 3657 (2010).
44. Z. Liu, L. Zhong, P. Ying, Z. Feng, C. Li. *Biophys. Chem.* **132**, 18 (2008).
45. G. Di Profio, S. Tucci, E. Curcio, E. Drioli. *Cryst. Growth Des.* **7**, 526 (2007).
46. T. N. Drebushchak, E. V. Boldyreva, Y. V. Seryotkin, E. S. Shutova. *J. Struct. Chem.* **43**, 835 (2002).
47. V. A. Drebushchak, E. V. Boldyreva, T. N. Drebushchak, E. S. Shoutova. *J. Cryst. Growth* **241**, 266 (2002).
48. E. S. Ferrari, R. J. Davey, W. I. Cross, A. L. Gillon, C. S. Towler. *Cryst. Growth Des.* **3**, 53 (2003).
49. H. Y. Yoshikawa, Y. Hosokawa, H. Masuhara. *Cryst. Growth Des.* **6**, 302 (2006).
50. G. Da Costa, J. Calatroni. *Appl. Opt.* **17**, 2381 (1978).
51. M. Gugliotti, M. S. Baptista, M. J. Politi. *Langmuir* **18**, 9792 (2002).
52. L. S. Sorell, A. S. Myerson. *AlChE J.* **28**, 772 (1982).
53. O. A. Louchev, S. Juodkazis, N. Murazawa, S. Wada, H. Misawa. *Opt. Exp.* **16**, 5673 (2008).
54. K. Kawahara, C. Tanford. *J. Bio. Chem.* **241**, 3228 (1966).
55. F. C. Meldrum, V. J. Wade, D. L. Nimmo, B. R. Heywood, S. Mann. *Nature* **349**, 684 (1991).
56. T. Douglas, M. Young. *Nature* **393**, 152 (1998).
57. K. Yoshizawa, Y. Mishima, S.-Y. Park, J. G. Heddle, J. R. H. Tame, K. Iwahori, M. Kobayashi, I. Yamashita. *J. Biochem.* **142**, 707 (2007).
58. S. Takeda, M. Ohta, S. Ebina, K. Nagayama. *Biochem. Biophys. Acta* **1174**, 218 (1993).
59. M. Okuda, K. Iwahori, I. Yamashita, H. Yoshimura. *Biotechnol. Bioeng.* **84**, 187 (2003).
60. A. Miura, R. Tsukamoto, S. Yoshii, I. Yamashita, Y. Uraoka, T. Fuyuki. *Nanotechnology* **19**, 255201 (2008).
61. R. Tsukamoto, K. Iwahori, M. Muraoka, I. Yamashita. *Bull. Chem. Soc. J.* **78**, 2075 (2005).
62. S. Masuo, H. Yoshikawa, H. G. Nothofer, A. C. Grimsdale, U. Scherf, K. Mullen, H. Masuhara. *J. Phys. Chem. B* **109**, 6917 (2005).
63. Y. Nabetani, H. Yoshikawa, A. C. Grimsdale, K. Mullen, H. Masuhara. *Jpn. J. Appl. Phys.* **46**, 449 (2007).

64. D. Gallant, M. Pezolet, S. Simard. *J. Phys. Chem. B.* **110**, 6871 (2006).
65. S. N. Kotsev, C. D. Duskin, I. K. Ilev, K. Nagayama. *Colloid Polym. Sci.* **281**, 343 (2003).
66. A. Miura, R. Tanaka, Y. Uraoka, N. Matsukawa, I. Yamashita, T. Fuyuki. *Nanotechnology* **20**, 12570 (2009).
67. T. Iida, H. Ishihara. *Phys. Rev. Lett.* **90**, 057403 (2003).
68. C. Hosokawa, H. Yoshikawa, H. Masuhara. *Jpn. J. Appl. Phys.* **45**, L453 (2006).

